# THEORETICAL ESTIMATION OF RAIN–WIND-INDUCED VIBRATIONS OF STAY CABLES CONSIDERING CABLE BENDING STIFFNESS AND AXIAL PRETENSION

**Hoang Trong Lam, Vo Duy Hung*, Phan Duc Tam, Nguyen Van My**

*The University of Danang – University of Science and Technology, Vietnam*

*Corresponding author: vdhung@dut.udn.vn

(Received: March 10, 2026; Revised: May 27, 2026; Accepted: June 05, 2026)

DOI: 10.31130/ud-jst.2026.24(7B).593E

**Abstract -** Rain–wind-induced vibration (RWIV) may produce large-amplitude, low-frequency oscillations in stay cables under combined wind and rainfall. This study presents a simplified analytical framework for estimating RWIV while explicitly considering axial pretension, bending stiffness, cable geometry, structural damping, and rivulet-induced aerodynamic effects. Based on quasi-steady galloping theory, the aerodynamic force is formulated by incorporating the initial position and harmonic motion of a water rivulet. The governing equation of a tensioned cable is solved using modal decomposition. Parametric analyses show that the predicted vibration amplitude increases with cable length and diameter, whereas greater axial pretension and natural frequency reduce the response. Bending stiffness has only a minor influence within the investigated range, confirming the tension-dominated behavior of slender stay cables. Application to an assumed cable-stayed bridge demonstrates that considerable RWIV may occur under unfavorable wind–rain conditions and highlights the need to consider cable dynamic properties in preliminary vibration assessment.

**Key words -** RWIV; Stay cable; theoretical model; pretension; bending stiffness

## 1. Introduction

Rain–wind-induced vibration (RWIV) is a major aerodynamic concern for stay cables in cable-stayed bridges. When wind acts together with rainfall, inclined cables can experience pronounced low-frequency oscillations with relatively large amplitudes. These vibrations may reduce bridge serviceability, accelerate fatigue damage, and affect the long-term safety and durability of the cable system. Since the widely cited observations on the Meiko-Nishi Bridge, RWIV has been recognized as a distinct form of environmental excitation in cable-supported structures, especially for long, slender, and lightly damped stay cables [1, 2].

The basic mechanism of RWIV is generally attributed to the development of rainwater rivulets along the cable surface. During rainfall, water accumulates on the upper and lower parts of the cable, altering its effective cross-sectional shape and consequently modifying the aerodynamic force coefficients. Among these features, the upper rivulet is generally considered the dominant contributor to instability because its position is highly sensitive to wind action, gravity, surface tension, and cable motion. The resulting interaction between cable vibration and rivulet movement changes the instantaneous aerodynamic loading and may produce negative aerodynamic damping, thereby triggering self-excited oscillations [2–5]. Later studies further confirmed that the dynamic behavior of water rivulets is not merely a secondary phenomenon but a central component of the excitation mechanism governing RWIV [6, 7].

Previous studies on RWIV have been conducted through field observations, wind-tunnel experiments, analytical models, numerical simulations, and review-based syntheses. Early field and experimental studies showed that RWIV typically occurs within a limited range of wind velocities and yaw angles and that the response is often dominated by low-order vibration modes with amplitudes large enough to threaten cable durability and anchorage performance [1, 2, 8]. Experimental investigations also demonstrated that the onset and amplitude of RWIV are closely related to rivulet formation, rivulet position, and cable surface conditions [3, 4, 9]. Furthermore, combined numerical and experimental studies have provided deeper insight into the aerodynamic forces acting on rain-covered stay cables and clarified how these forces vary with rivulet configuration and cable motion [10].

On the theoretical side, several analytical models have been proposed to explain the growth mechanism of RWIV. Yamaguchi [5] developed one of the early analytical descriptions of the instability of rain-exposed cables, while Xu and Wang [8] formulated a single-degree-of-freedom analytical model for RWIV. Wilde and Witkowski [9] subsequently proposed a simplified analytical representation that contributed to clarifying the principal parameters governing the phenomenon. More recently, Gao et al. [11] established a quasi-steady-state approximation for RWIV and demonstrated that the coupled interaction among cable motion, rivulet movement, and aerodynamic loading can be interpreted within a unified theoretical framework. Their critical review further emphasized the decisive role of dynamic water rivulets and summarized the current understanding of their contribution to RWIV excitation [7]. Although these theoretical approaches inevitably involve simplifying assumptions, they remain valuable for identifying the main controlling parameters and estimating the vibration response of stay cables under combined wind–rain action [5, 8, 11].

Numerical simulations have also become a useful approach for examining RWIV mechanisms and potential control measures. Bi et al. [12] analyzed the coupled rain–

wind response of stay cables and found that the interaction between cable motion and rivulet development plays a key role in generating large-amplitude vibration. In a further study, Bi et al. [13] examined stay cables equipped with longitudinal ribs and showed that surface modifications can substantially influence rivulet behavior and the resulting vibration response. These findings indicate that both structural properties and surface geometric details may significantly affect RWIV susceptibility [12, 13]. In parallel, research focusing on rainwater rivulets has improved the understanding of rivulet kinematics and aerodynamic interaction. For example, Lemaitre et al. [6] investigated rainwater rivulets on a cable subjected to wind, providing valuable physical insight into rivulet motion, while Li et al. [14] further examined the vibration characteristics of RWIV in stay cables and reinforced the importance of aerodynamic–hydrodynamic coupling.

Despite the extensive body of previous work, the influence of several structural parameters has not yet been fully clarified in simplified theoretical estimation frameworks suitable for engineering applications. Therefore, the present study does not aim to propose a new fundamental theory of RWIV but rather to provide a simplified engineering-oriented estimation framework in which cable bending stiffness and axial pretension are explicitly included in the stay-cable vibration equation. In practical bridge design, parameters such as cable length, mass, diameter, axial pretension, bending stiffness, natural frequency, and vibration mode directly determine the dynamic characteristics of stay cables and may therefore substantially influence RWIV amplitude [2, 5, 8, 11, 14].

Among these parameters, pretension and bending stiffness are particularly important because they affect both the modal properties and the overall vibration sensitivity of long cables. Previous research on stay-cable vibration control showed that cable bending stiffness can influence the dynamic characteristics of the cable–damper system and should be considered when estimating damper performance and vibration stability [15]. However, the effects of pretension and bending stiffness are often treated only indirectly or are insufficiently emphasized in simplified RWIV models. This limitation reduces the applicability of existing formulations when preliminary assessment or parametric evaluation is required in engineering practice. Recent work on the damping required to control RWIV has further highlighted the need for practical predictive tools capable of relating cable properties to vibration amplitude and vibration-control requirements [16].

Motivated by this issue, the present study develops a simplified theoretical model for estimating the rain–wind-induced vibration response of stay cables while explicitly considering axial pretension and cable bending stiffness. Based on galloping theory, the aerodynamic force acting on a rain-exposed cable is formulated by accounting for the effect of a water rivulet on the cable surface. The governing vibration equation is solved analytically using the method of separation of variables, allowing the cable response to be estimated under selected wind–rain conditions. Parametric analyses are then conducted to examine the effects of cable mass, diameter, length, pretension force, bending stiffness, natural frequency, and vibration mode on the predicted RWIV amplitude. Finally, the model is applied to an assumed cable-stayed bridge to provide a preliminary assessment of possible large-amplitude vibration and to discuss the parameters relevant to RWIV control.

## 2. Theoretical simulation of RWIV of stay cables considering stiffness and axial pretension

### *2.1. Equation of Vibration for Stay Cables Under the Influence of External Forces*

The transverse vibration of the stay cable under wind–rain aerodynamic excitation is modeled as a tensioned beam. The governing equation can be written as:

$$m\,\frac{\partial^2 y(x,t)}{\partial t^2} + c\,\frac{\partial y(x,t)}{\partial t} + EJ\,\frac{\partial^4 y(x,t)}{\partial x^4} - S\,\frac{\partial^2 y(x,t)}{\partial x^2} = F(x,t) \tag{1}$$

where y(x,t) is the vertical displacement of the cable in the vibration plane (m), x is the coordinate along the cable length (m), t is time (s), m is the mass of the cable per unit length (kg/m), c is the damping coefficient per unit length (N.s/m²), EJ is the bending stiffness of the cable (N.m²), S is the axial pretension force in the cable (N), and F(x,t) is the aerodynamic force per unit length acting on the cable due to wind–rain interaction (N/m).

For convenience, Eq. (1) may also be expressed in normalized form by dividing all terms by $m$:

$$\partial^2 \frac{y(x,t)}{\partial t^2} + 2\xi s\,\frac{\partial y(x,t)}{\partial t} + a^2\,\frac{\partial^4 y(x,t)}{\partial x^4} - 2s^2\,\frac{\partial^2 y(x,t)}{\partial x^2} = \frac{F(x,t)}{m} \tag{2}$$

where $a^2 = EJ/m$, $2s^2 = S/m$, and $\xi_s$ represents the equivalent damping parameter used in the analytical formulation.

### *2.2. Calculation of Aerodynamic Forces Due to Wind-Rain Effects*

#### *2.2.1. Calculation Steps*

In this study, the vibration response of a stay cable subjected to combined wind and rain effects is modeled theoretically. The inherent dynamic properties of the cable are assumed to be known, including the circular frequency $\omega$, mass per unit length $m$, and structural damping ratio $\xi_S$. Therefore, the main task is to determine the aerodynamic force $F$ in the cable vibration equation by considering the coupled interaction between wind flow and the rainwater rivulet formed on the cable surface. The calculation procedure is described as follows.

Step 1: Determine the wind speed and wind direction acting in the cable vibration plane. The cable position relative to the incoming wind is defined by the cable inclination angle $\alpha_0$ and the yaw angle $\beta$, which are used to transform the incoming wind into the effective wind component acting on the cable.

Step 2: Calculate the relative wind speed U_rel and the corresponding effective attack angle, considering the position of the rainwater rivulet on the cable surface, as shown in Figure 1. The rivulet modifies the aerodynamic profile of the cable and changes the resulting drag and lift forces.

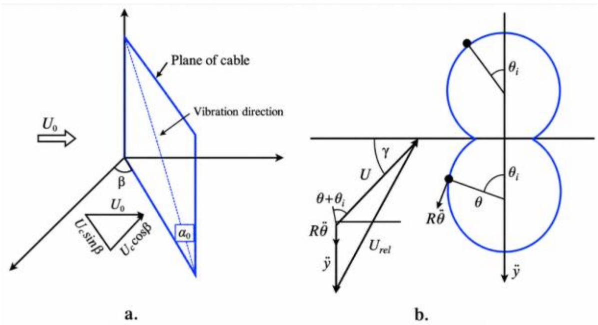


***Figure 1.*** *Cable position and wind direction of action*

Step 3: Assume that the oscillation of the rainwater on the cable $\theta$ follows a harmonic function: $\theta = a_m sin(\omega t)$;

Where: $a_m(U_0) = a_1.exp\left(-\frac{(U_0-U_{max})2}{a_2}\right)$; $a_1$, $a_2$, and $U_{max}$ depend on cable surface type.

The aerodynamic force is evaluated as a function of the relative wind speed, cable diameter, and air density. In general, the force per unit cable length can be expressed as:

$$F = \frac{U_{rel}^2 D\rho}{2}(C_L(\phi_e)\cos\varphi^* + C_D(\phi_e)\sin\phi^*) \tag{3}$$

where, D is the cable diameter, ρ is the air density, $C_L$ is the lift coefficient, and $C_D$ is the drag coefficient. The effective attack angle $\phi_e$ is defined as: $\phi_e = \phi^* - \theta - \theta_i$, where $\phi^*$, θ, and $\theta_i$ are the wind-related angle, the instantaneous rivulet angle, and the initial rivulet position, respectively, as illustrated in Figure 1.

*2.2.2. Estimation of aerodynamic forces*

To simplify the modeling and calculation of stay-cable vibration under combined wind and rain effects, several assumptions are adopted. First, the cable is assumed to undergo small-amplitude vibration with small deflection within the vibration plane. Second, the water rivulet is assumed to oscillate with the same dominant frequency as the stay cable. This assumption simplifies the analytical formulation for steady-state low-frequency RWIV, although actual rivulet motion may involve phase lag, nonlinear movement, and amplitude variation relative to the cable motion. Rainfall intensity is not explicitly included as an independent variable; its effect is indirectly represented by the assumed formation and initial position of the water rivulet on the cable surface. The vibration amplitude and initial position of the water rivulet are considered to vary with wind speed. The weight of the rivulet is neglected because it is much smaller than the self-weight of the cable. Finally, only low-frequency vibration modes are considered in the present model.

Consider a stay cable subjected to wind with a velocity of $U_o$, with an inclination determined by two angles $\alpha_o$ and β (see Figure 1). At this point, $U_o$ is divided into two components: The component $U_o cos\beta$, which acts perpendicular to the cable plane and the component $U_o sin\alpha_o$, which acts within the plane of the cable. The effect of this component on the cable is $U_o sin\alpha_o.sin\beta$.

Thus, the influence of wind speed and the angle of attack in the plane of vibration of the cable is:

$$U = U_0.\sqrt{cos^2\beta + sin^2\alpha_0 . sin^2\beta} \tag{4}$$

$$\gamma = \varepsilon\, sin^{-1}\left(\frac{sin\,\alpha_0.sin\,\beta}{\sqrt{cos^2\beta + sin^2\alpha_0.sin^2\beta}}\right) \tag{5}$$

To reflect the influence of the wind attack angle under rainy conditions in the right-hand side of equation 5, we add a coefficient $\varepsilon$. When $\varepsilon = 1$, it means that the cable's oscillation occurs without the presence of the water rivulet. When $\varepsilon = 0$, it means there is no water rivulet, and the wind attack angle $\beta = 0$.

The aerodynamic force depends on the wind coefficients, the actual wind velocity $U_{rel}$, and the corresponding attack angle, which is determined by the following formula:

$$U_{rel} = \sqrt{\left(R\frac{\partial\theta}{\partial t}sin(\theta+\theta_i) + U\,sin\,\gamma + \frac{\partial y}{\partial t}\right)^2 + \left(R\frac{\partial\theta}{\partial t}cos(\theta+\theta_i) + U\,cos\,\gamma\right)^2} \tag{6}$$

$$\phi^* = arctan\left(\frac{R\frac{\partial\theta}{\partial t}sin(\theta+\theta_i)+U\,sin\,\gamma+\frac{\partial y}{\partial t}}{R\frac{\partial\theta}{\partial t}cos\left(\theta+\frac{\partial\theta}{\partial t}\right)+U\,cos\,\gamma}\right) \tag{7}$$

Where R: cable radius, $\theta_i$: Initial position of the rainwater on the cable.

In that case, the aerodynamic force is calculated as follows:

$$F = \frac{U_{rel}^2 D\rho}{2}(C_L(\phi_e)\cos\phi^* + C_D(\phi_e)\sin\phi^*)0 \tag{8}$$

In the present simplified analytical model, the aerodynamic coefficients $C_L$ and $C_D$ are not treated as universal constants. They depend on the effective wind attack angle and the position of the water rivulet on the cable surface. These coefficients are obtained from published experimental results for rain-covered stay cables reported by Yamaguchi [5] and Gu and Du [2]. For use in the present calculation, the experimental aerodynamic-coefficient curves are locally linearized within the considered range of attack angle and rivulet position. Therefore, $C_L$ and $C_D$ are regarded as functions of the effective aerodynamic condition, rather than fixed values. This treatment is suitable for preliminary theoretical estimation, although it cannot fully describe the nonlinear and time-dependent behavior of the water rivulet.

By solving equation 8, we obtain the aerodynamic force as follows:

$$F(t) = F_1.sin(\omega t) + F_2.cos(\omega t) + F_3.sin(2\omega t) + F_4.cos(3\omega t) \tag{9}$$

Where: $F_1 = -\frac{1}{2}.U^2 D\rho.C_1.a_m$

$$F_2 = URD\rho.a_m.\left[cos\,\alpha.(\alpha C_1 + C_2) - \frac{1}{4}a_m^2.\omega.sin\,\alpha.C_1\right]$$

$$F_3 = \frac{1}{2}URD\rho.a_m^2.\omega.[sin\,\alpha.(\alpha C_1 + C_2) - cos\,\alpha.C_1]$$

$$F_4 = \frac{1}{4}URD\rho.a_m^3.\omega.sin\,\alpha.C_1$$

### *2.3. Solution of the vibration equation of a stay cable under combined wind–rain interaction*

The vibration equation (1) can be written as:

$$\frac{\partial^2 y}{\partial t^2} + 2\xi_s \frac{\partial y}{\partial t} + a^2 \frac{\partial^4 y}{\partial x^4} - 2s^2 \frac{\partial^2 y}{\partial x^2} = -\frac{F(t)}{m} \quad (10)$$

For the present preliminary analytical estimation, the stay cable is idealized as a simply supported tensioned member. Therefore, the transverse displacement and bending moment at both cable ends are assumed to be zero. The boundary conditions are expressed as:

$$y(0,t) = 0;\ y(L,t) = 0;$$

$$M(0,t) = EJ\,\partial^2 \frac{y(0,t)}{\partial x^2} = 0;$$

$$M(L,t) = EJ\,\partial^2 \frac{y(L,t)}{\partial x^2} = 0.$$

Where L is the cable length and M is the bending moment. This simplified boundary condition is adopted to obtain an analytical solution for preliminary RWIV estimation. In actual bridges, the cable anchorages may have more complex restraint conditions; therefore, this assumption is recognized as a limitation of the present model.

In the present model, cable sag is neglected, and the stay cable is simplified as a straight inclined tensioned member. This assumption is adopted to keep the analytical formulation suitable for preliminary estimation. It is acceptable when the sag-to-span ratio is relatively small and the axial pretension is sufficiently large. However, for very long stay cables, cable sag may influence the modal properties and vibration response; therefore, sag effects should be included in future refined analysis.

The initial conditions, taking $t_0 = 0$, are expressed as: $y(x,0) = 0, \dot{y}(x,0) = 0$. The governing differential equation is then solved using Bernoulli's method of separation of variables. Accordingly, the general solution for the vibration response of the stay cable under combined wind and rain action can be written as follows:

$$y(x,t) = \sin\left(\frac{n.\pi}{L}x\right).\{e^{-\xi_s.t}.\left[P_1.\cos\left(\sqrt{\omega^2 - \xi_s^2}.t\right) + P_2.\sin\left(\sqrt{\omega^2 - \xi_s^2}.t\right)\right] + \frac{F_1}{\omega.(2m\xi_s)}.\cos(\omega t) - \frac{F_2}{\omega.(2m\xi_s)}\sin(\omega t) + \frac{3F_3}{9m.\omega^2 + 16\xi_s^2}\sin(2\omega t) + \frac{4F_3.\xi_s}{\omega.(9m\omega^2 + 16\xi_s^2)}\cos(2\omega t) + \frac{2.F_4}{m.(16.\omega^2 - 9.\xi_s^2)}.\cos(3\omega t) + \frac{3F_5.\xi_s}{\omega.m.(32.\omega^2 - 18.\xi_s^2)}.\sin(3\omega t)\} \quad (11)$$

Where:

$$A_1 = UD\rho.\sin\gamma.[\alpha.C_1 + C_2];$$

$$C_1 = L_1.\cos\gamma + D_1.\sin\gamma;$$

$$C_2 = L_2.\cos\gamma + D_2.\sin\gamma;\ \gamma - \theta_i = \alpha;$$

$$\omega_n = \frac{n.\pi.a}{L}\sqrt{\frac{n^2.\pi^2}{L^2} + \frac{2s^2}{a^2}};\ a = \sqrt{\frac{EJ}{m}};\ s = \sqrt{\frac{S}{2m}};$$

Where: S is the axial tension force in the cable (N), m is the mass per unit length of the cable (kg/m), L is the cable length (m), EJ is the bending stiffness of the stay cable (N.m²), and n is the vibration mode number considered in the analytical solution.

## 3. Example calculation of combined wind-rain induced vibration

Based on the governing equation, the stay-cable response under combined wind and rain action can be expressed as a harmonic function. The vibration amplitude depends on key parameters such as natural frequency, cable mass, diameter, wind speed, cable inclination, wind direction, and the initial position of the water rivulet. Therefore, the following analysis examines the influence of these parameters to identify unfavorable conditions for RWIV.

### *3.1. Input the parameters:*

The stay cable and rain-rivulet conditions are assumed as follows: cable length L = 110 m, mass per unit length m = 100 kg/m, axial pretension S = 5000 kN, wind velocity $U_o$= 15 m/s, cable diameter D = 0.127 m, initial rainwater angle $\theta_0$ = 15°, air density $\rho$ = 1.225 kg/m³, wind attack angle $\alpha_o$ = 22.82°, and water rivulet angle $\beta$ = 45°. The structural damping ratio used in the calculation is $\xi_s$ = 0.2%. Damping directly affects the predicted RWIV amplitude because it controls the balance between aerodynamic excitation and structural energy dissipation. A lower damping ratio allows the vibration amplitude to grow more rapidly and reach a larger steady-state value, whereas a higher damping ratio suppresses the cable response. Therefore, the calculated amplitude should be interpreted together with the assumed damping level.

These parameters are selected to represent a typical medium-to-long stay cable in a cable-stayed bridge. The cable length, diameter, mass per unit length, and pretension force are within the practical range of stay-cable properties. The wind speed of 15 m/s is used because RWIV is commonly associated with moderate wind speeds under rainfall. The selected wind attack angle and rivulet position represent an unfavorable wind–rain condition for preliminary RWIV assessment, rather than a specific bridge case.

### *3.2. Calculation RWIV of stay cable*

Consider the first vibration mode, n = 1, and investigate the response at the midspan position x = L/2. The first vibration mode is selected because RWIV of stay cables is generally associated with low-frequency, large-amplitude vibration. For long stay cables, lower modes usually have smaller natural frequencies and are more easily excited under wind–rain interaction. Therefore, the first mode is considered critical for the preliminary RWIV assessment in this study. The vibration equation becomes:

$$y\left(\frac{L}{2},t\right) = e^{-\xi_s.t}.\left[P_1.cos\left(\sqrt{\omega^2-\xi_s{}^2}.t\right)+ P_2.sin\left(\sqrt{\omega^2-\xi_s{}^2}.t\right)\right] + \frac{F_1}{\omega.(2m\xi_s)}.cos(\omega t) - \frac{F_2}{\omega.(2m\xi_s)}sin(\omega t) + \frac{3F_3}{9m.\omega^2+16\xi_s{}^2}sin(2\omega t) + \frac{4F_3.\xi_s}{\omega.(9m\omega^2+16\xi_s{}^2)}cos(2\omega t) + \frac{2.F_4}{m.(16.\omega^2-9.\xi_s{}^2)}.cos(3\omega t) + \frac{3F_4.\xi_s}{\omega.m.(32.\omega^2-18.\xi_s{}^2)}.sin(3\omega t) \quad (12)$$

From the boundary condition: $y_0 = 0$ (m); $y'_0 = 0$, $P_1$ and $P_2$ can be calculated by:

$$P_1 = -\left[\frac{F_1}{\omega.(2m\xi_s)} + \frac{4F_3.\xi_s}{\omega.(9m\omega^2+16\xi_s{}^2)} + \frac{2.F_4}{m.(16.\omega^2-9.\xi_s{}^2)}\right] \quad (13)$$

$$P_2 = \frac{1}{\sqrt{\omega^2-\xi_s{}^2}}\left[\frac{F_2}{(2m\xi_s)} - \frac{6\omega F_3}{9m.\omega^2+16\xi_s{}^2} - \frac{9F_4.\xi_s}{m.(32.\omega^2-18.\xi_s{}^2)}\right] \quad (14)$$

In the present analytical framework, RWIV is considered likely to occur when the aerodynamic excitation associated with the rainwater rivulet overcomes the structural damping of the cable. This condition is related to negative aerodynamic damping and is controlled by the combined effects of wind velocity, wind attack angle, rivulet position, aerodynamic-force gradient, cable frequency, and structural damping. Therefore, RWIV occurrence is not determined by wind speed alone, but by the coupled wind–rain–cable interaction.

Figures 2 and 3 show the calculated vibration response and aerodynamic force of the stay cable under combined wind–rain action. Figure 2 indicates a harmonic cable response caused by periodic aerodynamic excitation from wind flow and the rainwater rivulet. The vibration amplitude increases rapidly during the first 100 s and then approaches a stable response after about 600–700 s. The maximum amplitude reaches approximately 0.9 m, indicating a severe RWIV response for the assumed long and lightly damped cable. This value is consistent with the possible order of large-amplitude vibration reported in previous studies [1, 2, 6, 7], but it should be interpreted as an unfavorable theoretical estimate rather than a direct prediction for a specific bridge. Figure 3 shows that the aerodynamic force fluctuates periodically around 14.6 N/m, ranging from approximately 13.4 to 14.8 N/m.

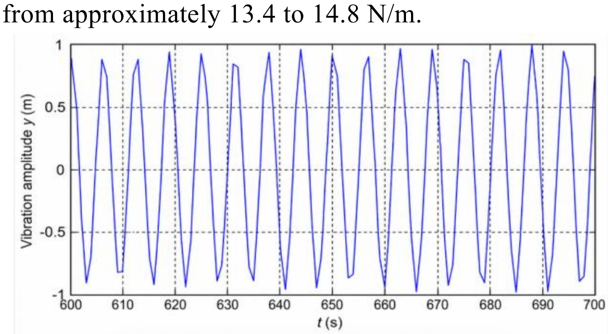


***Figure 2.*** *Time history of stay-cable vibration under combined wind–rain interaction*

Figure 4 presents the predicted vibration amplitudes of the assumed stay cables with different geometric and mechanical properties. In the investigated bridge model, the cable length ranges from 34 m to 156 m, the mass per unit length from 40 kg/m to 100 kg/m, the cable diameter from 0.08 m to 0.13 m, the bending stiffness from 8.40 × 10^7 to 5.08 × 10^8 N·m², and the pretension force from 4653.8 kN to 7702.3 kN. The calculated amplitudes range from 28.5 cm to 74.17 cm, showing that considerable RWIV may occur under unfavorable wind–rain conditions, especially for relatively long and flexible cables. These results indicate the need for RWIV mitigation measures, such as external dampers, surface treatments, or pretension adjustment.

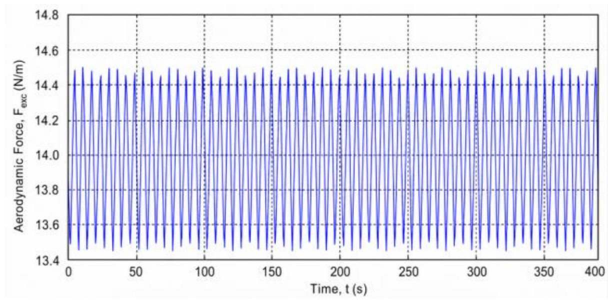


***Figure 3.*** *Time history of aerodynamic force acting on the stay cable under combined wind–rain interaction.*

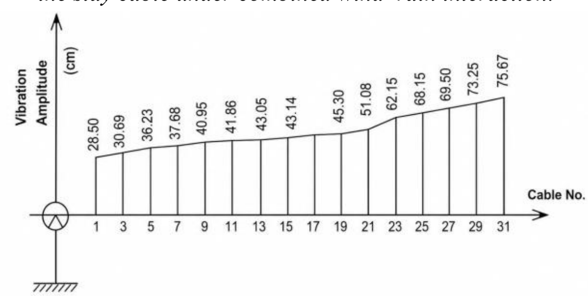


***Figure 4.*** *Predicted RWIV amplitudes of the stay cables*

### *3.3. Parametric study*

*3.3.1. Relationship between cable mass and vibration amplitude*

To investigate the effect of cable mass on RWIV response, three mass values are considered: m = 80, 100, and 120 kg/m, as shown in Figures 5–7. The results indicate that changing the mass per unit length has only a limited effect on the maximum vibration amplitude. In all three cases, the peak amplitude remains approximately 0.9 m. However, a smaller cable mass causes the response to reach its steady-state amplitude more rapidly, indicating that lighter cables may be more sensitive to the growth stage of RWIV.

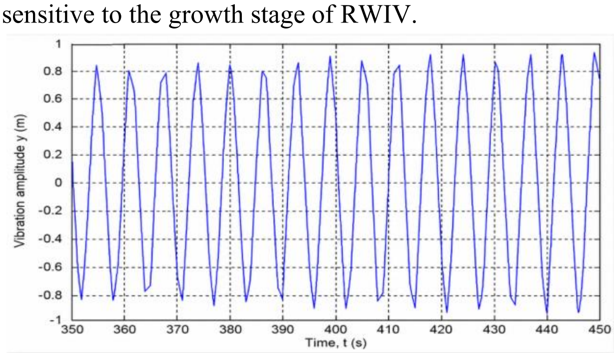


***Figure 5.*** *Time history of cable vibration for m = 80 kg/m*

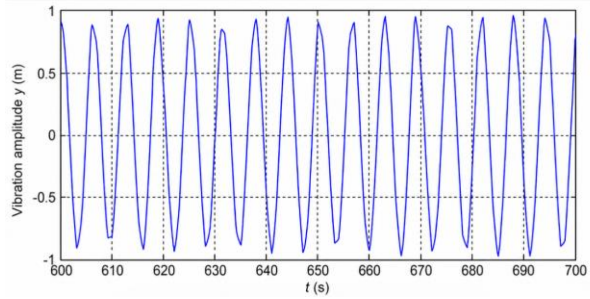


***Figure 6.*** *Time history of cable vibration for m = 100 kg/m*

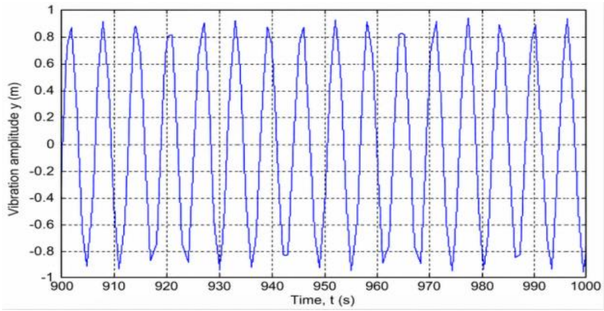


***Figure 7.*** *Time history of cable vibration for m=120kg/m*

### *3.3.2. Relationship between cable diameter (D) and vibration amplitudes*

To evaluate the effect of cable diameter on vibration response, three diameters were considered: D = 0.0827 m, 0.127 m, and 0.147 m. The corresponding time-history responses are shown in Figures 8–10. The results show that the cable undergoes sustained periodic vibration in all cases. The vibration amplitude increases with increasing cable diameter. For D = 0.0827 m, the peak amplitude is about ±0.6 m, while it increases to nearly ±0.9 m for D = 0.127 m and exceeds ±1.0 m for D = 0.147 m. This trend indicates that larger cable diameters lead to stronger wind–rain-induced vibration, likely due to the increased aerodynamic surface and enhanced interaction between wind, rain rivulets, and the cable. Therefore, cable diameter is an important parameter in assessing and controlling cable vibration.

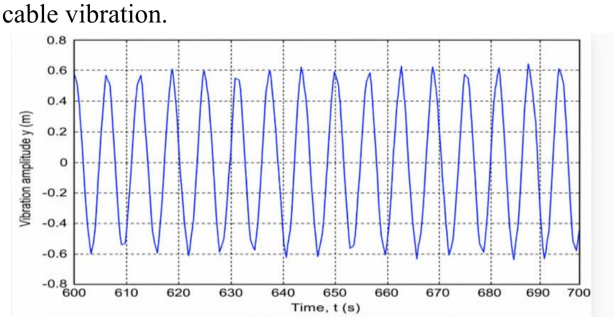


***Figure 8.*** *Time history of cable vibration for D=0.0827m*

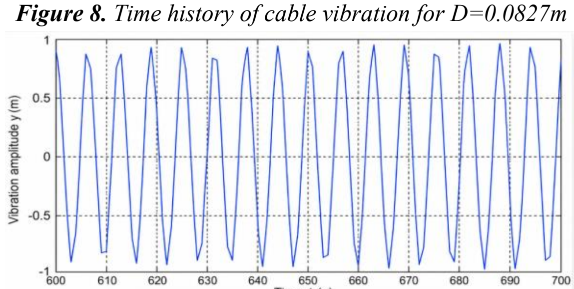


***Figure 9.*** *Time history of cable vibration for D=0.127m*

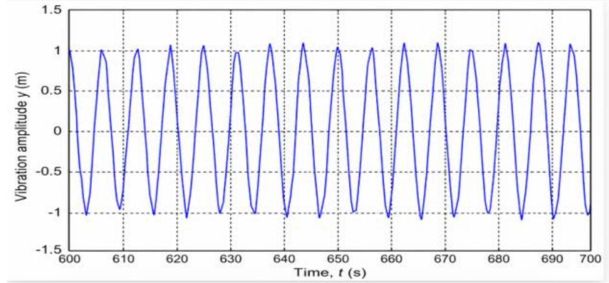


***Figure 10.*** *Time history of cable vibration for D=0.147m*

### *3.3.3. Factors affecting the natural frequency of stay cable*

The natural frequency of the stay cable subjected to combined wind and rain is calculated according to equation:

$$\omega_n = \frac{n.\pi.a}{L}\sqrt{\frac{n^2.\pi^2}{L^2} + \frac{2s^2}{a^2}} \tag{15}$$

According to the frequency expression, the fundamental natural frequency of the stay cable is governed by axial tension, mass per unit length, cable length, and bending stiffness, which determine the effective stiffness and inertia of the cable system. A parametric investigation is therefore conducted for the first vibration mode, n=1, which is particularly relevant to large-amplitude cable vibration. Figures 11–13 present the effects of axial pretension S, bending stiffness EJ, and cable length L on the fundamental natural frequency.

As shown in Figure 11, the natural frequency increases with axial pretension because higher tension improves the cable's resistance to transverse deformation. The nonlinear trend indicates that the sensitivity of frequency to pretension gradually decreases at higher tension levels. Figure 12 shows that increasing bending stiffness EJ causes only a slight increase in natural frequency, confirming that the response of long, slender stay cables is mainly tension-dominated. Thus, bending stiffness has only a secondary influence within the investigated range. In contrast, Figure 13 shows that the natural frequency decreases significantly as cable length increases. Longer cables have lower global stiffness and greater flexibility, resulting in lower vibration frequencies. Overall, axial pretension and cable length are the dominant parameters controlling the fundamental natural frequency, whereas bending stiffness has a comparatively minor effect. These findings emphasize the importance of accurately defining cable tension and length in stay-cable dynamic analysis and vibration-control design.

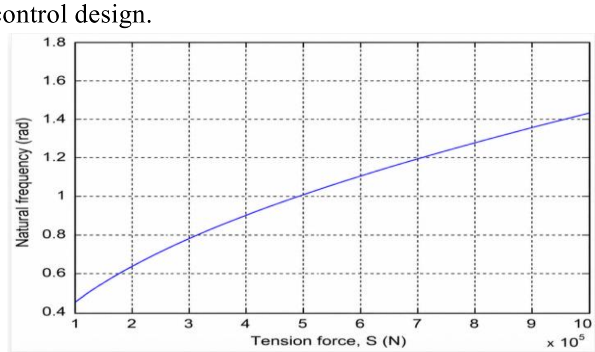


***Figure 11.*** *Effect of axial pretension on the fundamental frequency*

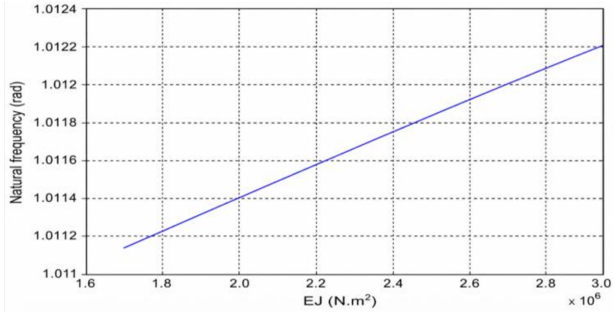


***Figure 12.*** *Effect of bending stiffness on the fundamental frequency*

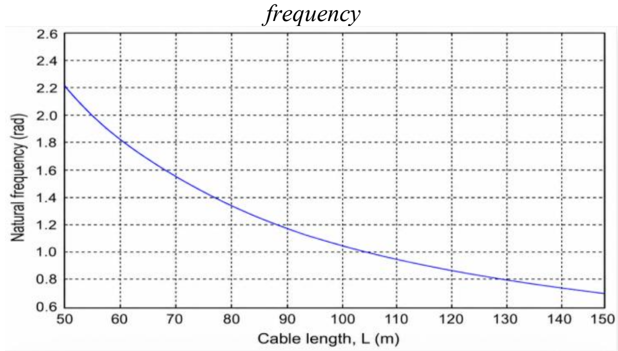


***Figure 13.*** *Effect of cable length on the fundamental frequency*

## 4. Conclusions

This study presented a simplified theoretical estimation of rain–wind-induced vibration of stay cables considering cable bending stiffness and axial pretension. The stay cable was modeled as a tensioned beam subjected to aerodynamic excitation caused by wind–rain interaction and water-rivulet effects. The numerical results show that large-amplitude RWIV may occur under unfavorable wind–rain conditions. For the assumed cable, the predicted maximum amplitude reaches approximately 0.9 m. In the hypothetical bridge example, the calculated amplitudes range from 28.5 cm to 74.17 cm. The parametric results indicate that cable length and diameter tend to increase vibration amplitude, while higher axial pretension and higher natural frequency reduce the response. The influence of bending stiffness on natural frequency is relatively small compared with the effects of cable length and axial pretension. These findings suggest that axial pretension, natural frequency, and damping should be considered in preliminary RWIV assessment of stay cables. Since the present model is simplified, further validation using wind-tunnel or field data is needed, especially to account for nonlinear rivulet motion, rainfall intensity, cable sag, and actual boundary conditions.

**Acknowledgments:** This research is funded by Funds for Science and Technology Development of the University of Danang under project number B2024-DN02-21.

## REFERENCES

[1] Y. Hikami and N. Shiraishi, “Rain-wind induced vibrations of cables stayed bridges,” *Journal of Wind Engineering and Industrial Aerodynamics*, vol. 29, no. 1, pp. 409–418, 1988.

[2] M. Gu and X. Q. Du, “Experimental investigation of rain-wind induced vibration of cables in cable-stayed bridges and its mitigation,” *Journal of Wind Engineering and Industrial Aerodynamics*, vol. 93, pp. 79–95, 2005.

[3] C. Verwiebe and H. Ruscheweyh, “Recent research results concerning the exciting mechanisms of rain-wind-induced vibrations,” *Journal of Wind Engineering and Industrial Aerodynamics*, vols. 74–76, pp. 1005–1013, 1998.

[4] U. Peil and N. Nahrath, “Modelling of rain-wind induced vibration,” *Wind and Structures*, vol. 6, no. 1, pp. 41–52, 2003.

[5] H. Yamaguchi, “Analytical study on growth mechanism of rain vibration of cables,” *Journal of Wind Engineering and Industrial Aerodynamics*, vol. 33, pp. 73–80, 1990.

[6] C. Lemaitre, M. M. Alam, and P. Hemon, “Rainwater rivulets on a cable subject to wind,” *Comptes Rendus Mécanique*, vol. 334, pp. 158–163, 2006.

[7] D. Gao et al., “Role of dynamic water rivulets in the excitation of rain–wind-induced cable vibration: A critical review,” *Advances in Structural Engineering*, vol. 24, no. 16, 2021. https://doi.org/10.1177/13694332211040136.

[8] Y. L. Xu and L. Y. Wang, “Analytical study of wind-rain-induced cable vibration: SDOF model,” *Journal of Wind Engineering and Industrial Aerodynamics*, vol. 91, nos. 1–2, pp. 27–40, 2003.

[9] K. Wilde and W. Witkowski, “Simple model of rain-wind-induced vibrations of stayed cables,” *Journal of Wind Engineering and Industrial Aerodynamics*, vol. 91, no. 7, pp. 873–891, 2003.

[10] H. Li, W. L. Chen, F. Xu, and F. C. Li, “A numerical and experimental hybrid approach for the investigation of aerodynamic forces on stay cables suffering from rain-wind-induced vibration,” *Journal of Fluids and Structures*, vol. 26, nos. 7–8, pp. 1195–1215, 2010.

[11] D. Gao, Z. Ning, Y. Duan, W. L. Chen, and H. Li, “Theory of rain-wind-induced vibration of stay cables: A quasi-steady-state approximation,” *Physics of Fluids*, vol. 34, no. 9, 2022. https://doi.org/10.1063/5.0112894.

[12] J. Bi, J. Wu, J. Guan, and J. Wang, “Numerical simulation of rain-wind-induced vibration of stay cables and its mechanism study,” *Journal of Vibration and Shock*, vol. 36, pp. 111–117, 2017. https://doi.org/10.13465/j.cnki.jvs.2017.11.017.

[13] J. H. Bi, H. Y. Qiao, N. Nikitas, J. Guan, J. Wang, and P. Lu, “Numerical modelling for rain-wind-induced vibration of cables with longitudinal ribs,” *Journal of Wind Engineering and Industrial Aerodynamics*, vol. 178, pp. 69–79, 2018. https://doi.org/10.1016/j.jweia.2018.05.002.

[14] Y. Li, Y. L. Xu, K. M. Shum, and B. Chen, “Rain-wind-induced vibration of cables in cable-stayed bridges (I): Mechanism analysis,” *Journal of Southwest Jiaotong University*, vol. 46, no. 4, pp. 529–534, 552, 2011. https://doi.org/10.3969/j.issn.0258-2724.2011.04.001.

[15] N. D. Thao, “Improving the vibration stability of stay cables using a viscoelastic damper considering cable bending stiffness,” *The University of Danang – Journal of Science and Technology*, vol. 10, no. 71, pp. 32–37, 2013.

[16] V. Pinto, C. Georgakis, A. Larsen, D. Bergman, and C. Demartino, “Required damping estimation for rain-wind-induced vibration of stay cables: A preliminary evaluation,” in *Proc. IABSE Congress Tokyo 2025*, Tokyo, Japan, 2025, pp. 1894–1901. https://doi.org/10.2749/tokyo.2025.1894.